

Supporting Information

Direct characterization of the native structure and mechanics of cyanobacterial carboxysomes

Matthew Faulkner,^a Jorge Rodriguez-Ramos,^a Gregory F. Dykes,^a Sian V. Owen,^a Selene Casella,^a Deborah M. Simpson,^a Robert J. Beynon^a and Lu-Ning Liu^{a,*}

^aInstitute of Integrative Biology, University of Liverpool, Liverpool L69 7ZB, United Kingdom. E-mail: luning.liu@liverpool.ac.uk.

Table S1 Proteomic results of isolated β -carboxysomes from Syn7942. The column of Normalized amount displays the amount of each of the carboxysomal proteins detected in isolated β -carboxysomes using mass spectroscopy, normalized against the amount of the least abundant protein CcmL.

Protein	Normalized amount (fmol)
RbcL	4530.8 \pm 432.8
RbcS	1744.5 \pm 765.1
CcmM	1567.1 \pm 412.8
CcmK2	116.6 \pm 22.0
CcaA	81.8 \pm 12.6
CcmK4	18.7 \pm 0.4
CcmL	1

Table S2 Comparison of the dimensions of isolated carboxysomes from different species using TEM.

Type	Species	Diameter (nm)	Range (nm)	Reference
α -carboxysome	<i>Halothiobacillus neapolitanus</i>	117.3 \pm 6.9	97 – 132	1
α -carboxysome	<i>Halothiobacillus neapolitanus</i>	100	88 – 108	2
α -carboxysome	<i>Halothiobacillus neapolitanus</i>	134 \pm 8	116 – 169	3
α -carboxysome	<i>Synechococcus</i> WH8102	123 \pm 5	114 – 137	4
α -carboxysome	<i>Prochlorococcus marinus</i> MED4	90	70 – 100	5
β -carboxysome	<i>Synechococcus elongatus</i> PCC7942	149.90 \pm 13.78	100 – 200	This study

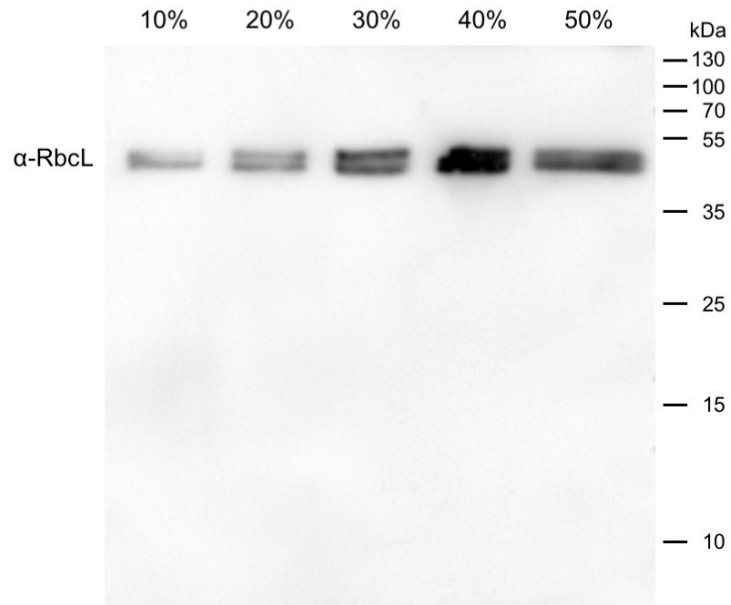


Fig. S1 Immunoblotting analysis of different β -carboxysome fractions using anti-RbcL antibody. Immunoblotting assays were carried out on the SDS-PAGE gel shown in Fig. 1C. RbcL (~50 kDa) was detected in all sucrose fractions and was most abundant in the 40 % sucrose fraction.

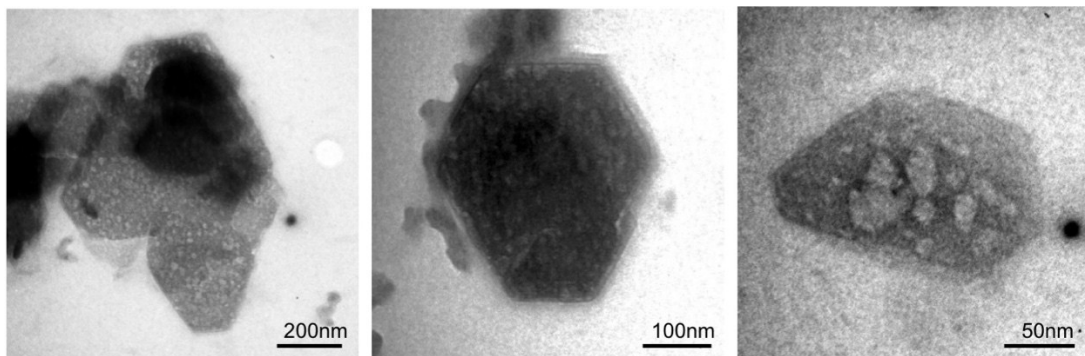


Fig. S2 TEM images of partial β -carboxysome fragments in the 20 and 30% sucrose fractions.

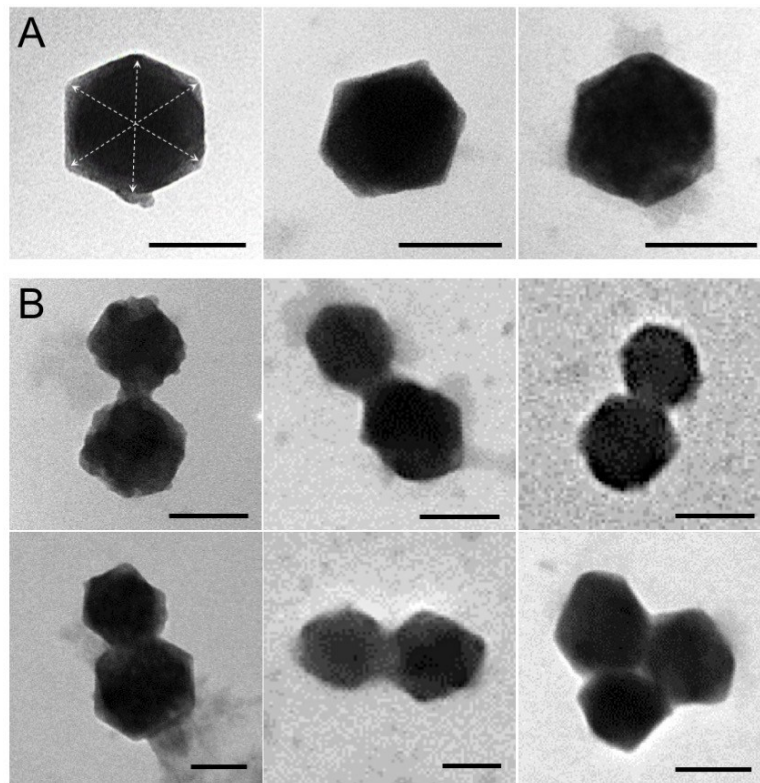


Fig. S3 TEM images of intact β -carboxysomes in the 40% sucrose fraction. (A) TEM images of individual intact β -carboxysomes. The dashed arrows represent the vertex-to-vertex measurements for determining the β -carboxysome diameter as described in Fig. 4B. (B) TEM images of β -carboxysome aggregations (Fig. 4C). Scale bar: 100 nm.

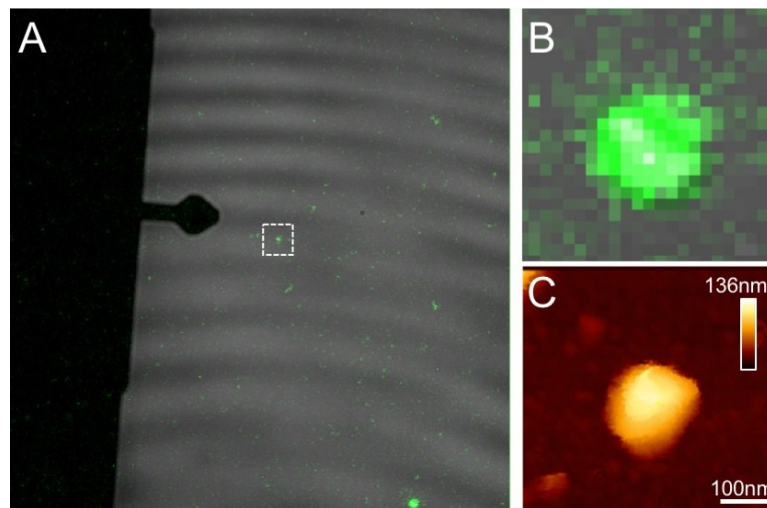


Fig. S4 Combined confocal and AFM imaging of β -carboxysomes fused with GFP. (A) A merged image of the transmitted and GFP channels captured using a hybrid JPK AFM-Zeiss 880 confocal microscope. The white dashed square represents a $10 \times 10 \mu\text{m}$ field of view of AFM after the engage. (B) Fluorescence image of a single β -carboxysome in the view highlighted by the white square in panel A. (C) AFM topograph of the same β -carboxysome captured simultaneously with the fluorescence image (B). The combination of AFM-confocal fluorescence imaging ensures the identification of β -carboxysomes on AFM substrate.

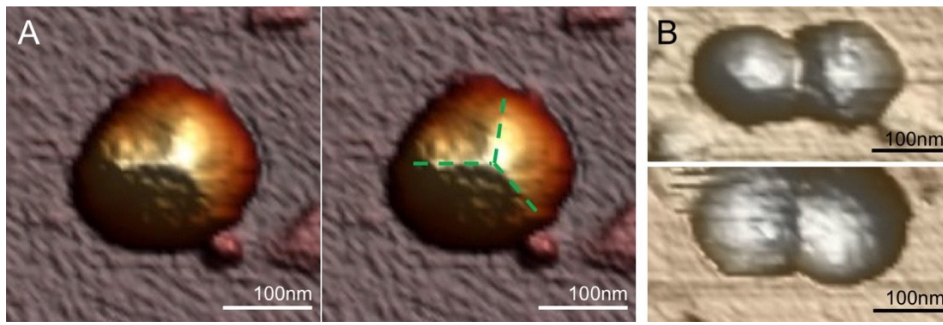


Fig. S5 AFM images of intact β -carboxysomes. (A) AFM topograph of single β -carboxysome with a vertex and three facet boundaries resolved, indicated by the green dashed lines. (B) AFM topographs of aggregated β -carboxysomes, reminiscent of EM results (Fig. 4C, Fig. S3B).

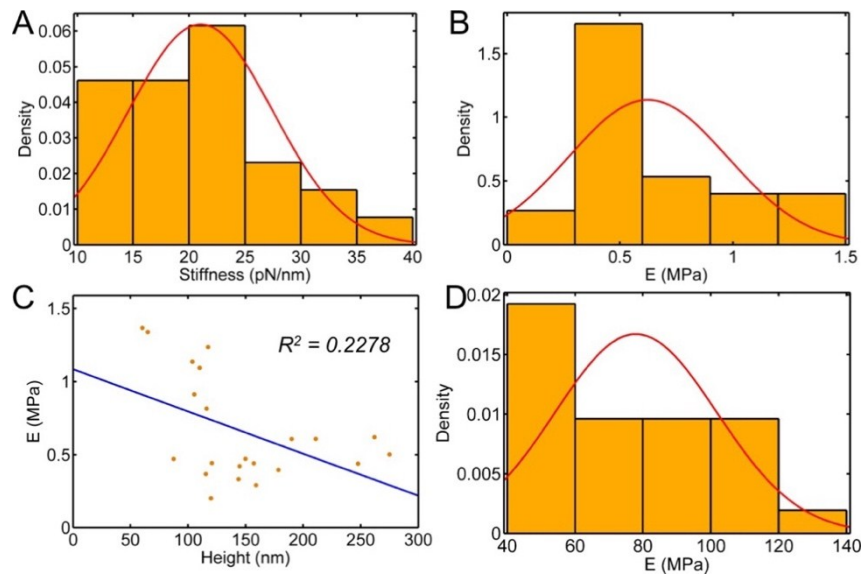


Fig. S6 Statistical analysis of the nanomechanical properties of β -carboxysomes. (A) Histogram of the β -carboxysome stiffness (k_{CB} , $n = 25$, Equation 1). (B) Histogram of Young's moduli of β -carboxysomes (E_H , $n = 20$) using the Hertzian model (Equation 3). (C) There is no correlation between Young's moduli and the carboxysome diameter ($y = -0.0039x + 1.1$, $R^2 = 0.2278$). (D) Histogram of Young's moduli of β -carboxysomes (E_S , $n = 25$) using the thin shell model (Equation 2).

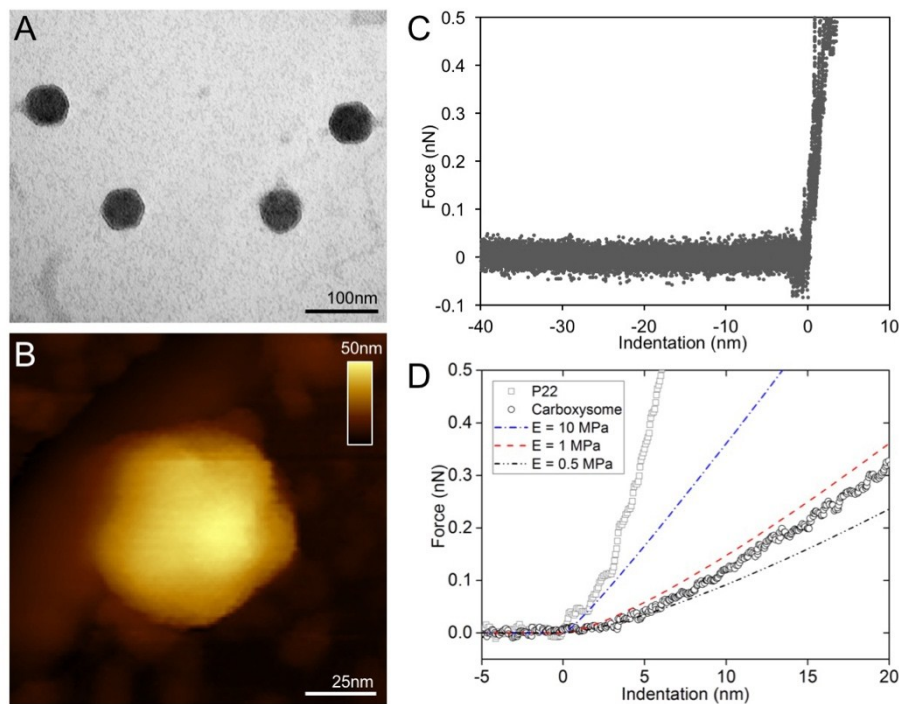


Fig. S7 Characterization of P22 particles. (A) TEM images of isolated P22 bacteriophage. (B) AFM topograph of a single P22 bacteriophage. The average height is 65.1 ± 5.9 nm ($n = 20$), in good agreement with previous AFM data.⁶ (C) Force-indentation curves of individual P22 particles. (D) The force-indentation curves of a single β -carboxysome (circle), a single P22 particle (square) and simulated force-indentation curves (colored dash lines) using a Hertz contact model in a sample with Young's moduli of 0.5, 1 and 10 MPa. The height of P22 particles is 65.1 ± 5.9 nm ($n = 20$) and the spring constant of P22 is approximately 192.38 ± 63.77 pN/nm ($n = 8$). Young's moduli of P22 fitted to the linear model and the Hertzian model are 101.04 ± 32.29 MPa and 11.06 ± 8.77 respectively ($n = 8$). Young's modulus of β -carboxysomes obtained using the Hertzian model ($E_H = 0.59 \pm 0.34$ MPa, $n = 20$) is significantly lower than those of P22, demonstrating the mechanical softness of β -carboxysome structures compared with P22.

Supporting References

1. Y. A. Holthuijzen, J. F. L. van Breemen, W. N. Konings and E. F. J. van Bruggen, *Archives of Microbiology*, 1986, **144**, 258-262.
2. M. F. Schmid, A. M. Paredes, H. A. Khant, F. Soyer, H. C. Aldrich, W. Chiu and J. M. Shively, *J Mol Biol*, 2006, **364**, 526-535.
3. C. V. Iancu, D. M. Morris, Z. Dou, S. Heinhorst, G. C. Cannon and G. J. Jensen, *J Mol Biol*, 2010, **396**, 105-117.
4. C. V. Iancu, H. J. Ding, D. M. Morris, D. P. Dias, A. D. Gonzales, A. Martino and G. J. Jensen, *J Mol Biol*, 2007, **372**, 764-773.
5. E. W. Roberts, F. Cai, C. A. Kerfeld, G. C. Cannon and S. Heinhorst, *J Bacteriol*, 2012, **194**, 787-795.
6. A. Llauro, D. Luque, E. Edwards, B. L. Trus, J. Avera, D. Reguera, T. Douglas, P. J. Pablo and J. R. Caston, *Nanoscale*, 2016, **8**, 9328-9336.